# Electrochemical measurements of the effects of inertial acoustic cavitation by means of a novel dual microelectrode

Peter R. Birkin [a,*], Douglas G. Offin [a], Timothy G. Leighton [b]

[a] *Department of Chemistry, University of Southampton, Southampton SO17 1BJ, UK*
[b] *Institute of Sound and Vibration Research, University of Southampton, Southampton SO17 1BJ, UK*

## Abstract

A novel dual microelectrode system has been developed to study the effects of cavitation at the solid/liquid interface. By sealing lead and platinum microelectrodes in close proximity, the mass transfer and surface effects from the same inertial cavitation event have been recorded simultaneously for the first time. A number of advantages of the system have been outlined. In addition supporting evidence for an erosion/corrosion mechanism on the lead electrode is reported.
© 2004 Elsevier B.V. All rights reserved.

*Keywords:* Cavitation; Ultrasound; Mass transfer; Erosion

## 1. Introduction

Irradiation of an electrode with ultrasound generated by horn-type transducers can have dramatic effects in terms of both enhanced mass transfer of electroactive species to the electrode [1–6] and erosion of the electrode surface [7–9]. In both cases the phenomenon of cavitation contributes greatly to the physical effects observed [10]. Mass transfer enhancement at sonicated microelectrodes is characterised by an increased steady-state current, due to acoustic streaming, superimposed with current spikes caused by the motion or collapse of cavitational bubbles. The exact nature of these current spikes is largely dependent on the electrode to horn separation. At small distances (<3 mm) single, transient current spikes have been observed [2,5,6], which have been associated with forced convection due to microjetting during inertial bubble collapse. At greater distances (up to 1 cm) periodic enhancements in mass transfer at

harmonics of the driving frequency have been seen by Maisonhaute et al. [11,12] and were attributed to periodic blocking of the electrode by an oscillating bubble. This change in behaviour is indicative of a transition from a region where inertial and non-inertial cavitation exists to a region where only non-inertial cavitation is present. This is due to a decrease in the acoustic pressure as the distance from the horn increases [13]. While mass transfer enhancement is sensitive to a myriad of mechanisms (acoustic streaming, inertial and non-inertial cavitation and other bubble motions), cavitation erosion can only be caused by the high-energy processes, such as microjetting and shockwave formation associated with inertial cavitation. Birkin et al. [8] used passivated lead and aluminium microelectrodes to record repassivation transients associated with erosion caused by single, inertial bubble collapses. Although the erosion and mass transfer effects of power ultrasound have been studied, each process is usually considered individually. The aim of this work is to use lead and platinum microelectrodes together to study the mass transfer and erosion effects of cavitation simultaneously. Lead was chosen to study erosion events as it can be easily

---

* Corresponding author. Tel.: +44 2380 594172; fax: +44 2380 593781.
*E-mail address:* prb2@soton.ac.uk (P.R. Birkin).

passivated, while platinum is an excellent material for probing mass transfer effects, using well-characterised redox reactions. A system of this type will provide a much greater insight into the nature of processes occurring within the plume of an ultrasonic horn.

## 2. Experimental

The basic experimental set-up for acoustoelectrochemical experiments has been described previously [5]. For this work a micrometer stage was added to enable movement in the XY plane of 25 mm in each direction with 10 μm resolution.

The Pb/Pt dual electrode was constructed by sealing lead microwire (125 μm diameter, 99.5%, Goodfellow) and an insulated platinum microwire (50 μm diameter, 99.99%, Goodfellow) in close proximity (ca. 100 μm centre to centre separation) within the same housing (a glass Pasteur pipette). This was achieved by the employment of a casting epoxy resin (Struers Epofix). Cyclic voltammetry was recorded using a home built potentiostat interfaced with a PC through an ADC card (Computer Boards, PCI-DAS 4020/12) and software written in-house. Platinum gauze served as the counter electrode and a saturated calomel electrode (SCE) or Ag wire (+0.04 V vs. SCE) was used as the reference or pseudo reference electrode, respectively (see appropriate figure legend). The Pb/Pb dual microelectrode was constructed in a similar manner to the Pb/Pt electrode. However, to insulate one of the 125 μm diameter Pb electrodes employed, a layer of lacquer was applied prior to assembly.

For acoustoelectrochemical experiments the current from both electrodes was recorded simultaneously by means of a dual current follower. The bandwidth [1] of the dual current follower employed (constructed using a TL071CP operational amplifier) in this work was 790 kHz for the erosion events (gain = $1 \times 10^4$ V A$^{-1}$) and 240 kHz for the mass transfer events (gain = $1 \times 10^5$ V A$^{-1}$). The rise time of the system was 13.7 and 374 A s$^{-1}$ for mass transfer and erosion measurements, respectively. These rise times were found to be faster than the electrochemical events detected in the presence of cavitation indicating that the events were not distorted by the associated measurement electronics. In the dual current follower experiments a silver wire was used as a counter/reference electrode and the current was recorded by a Tektronix TDS 220 digital oscilloscope at a sampling rate of 1 MHz.

Ultrasound and cavitation were generated by means of a Grundig Digimess FG 100 function generator, Brüel & Kjær Type 2713 power amplifier and ultrasonic

transducer fitted with a 3 mm diameter titanium tip (Adaptive Biosystems). The function generator was interfaced with a PC using software written in-house, allowing the frequency, input voltage and duration of the ultrasound to be accurately controlled. For this work continuous ultrasound was used (22.83 kHz). The ultrasound was characterised in terms of both the calorific intensity (56 ± 5 W cm$^{-2}$) and the acoustic pressure amplitude generated in the cell. The acoustic pressure amplitude (at the driving frequency) was determined by performing an FFT of the pressure signal from a hydrophone placed in the cell. At a distance of 11.2 mm from the tip of the horn the pressure amplitude was 11 ± 1 kPa. The pressure was measured at a large distance to minimise the effects of spatial averaging due to size of the sensing element in the hydrophone.

All solutions were made up using water from an USF Elga Purelab Option E10 water purification system (concentrations are given in the appropriate figure legend). Water purified in this manner had a conductivity of below 0.06 μS cm$^{-1}$ and a low organic content (TOC < 30 ppb [2]). Sodium sulphate (BDH, AnalaR) and potassium ferrocyanide (Aldrich, 99%) were used as supplied. Lead sulphate was made by precipitation of Pb(NO$_3$)$_2$ (Alfa Aesar Puratronic, 99.999%) in sodium sulphate. The solid PbSO$_4$ produced was washed with water and dried in an oven. Fresh solutions were used in all experiments to avoid problems associated with the oxidation of the ferrocyanide ion. All experiments were performed under aerobic conditions at 25 ± 1 °C.

## 3. Results and discussion

An SEM of the dual microelectrode after appropriate polishing is shown in Fig. 1. The close proximity of the microdiscs to each other is essential given the small diameter of cavitational bubbles expected [3] and the desire to quantify the cavitation processes occurring in the same volume of the liquid simultaneously. The voltammetry of both the microdiscs in a solution of 10 mM K$_4$Fe(CN)$_6$ and 0.75 M Na$_2$SO$_4$ is shown in Fig. 2. In the case of lead microelectrode (solid line), there is an oxidation peak at −0.45 V vs. SCE, due to the formation of a passivating PbSO$_4$ layer and a corresponding stripping peak at −0.70 V vs. SCE on the reverse scan. At potentials greater than −0.4 V vs. SCE the Pb microelectrode surface is covered with an insoluble PbSO$_4$ layer and essentially zero current was observed. The dotted line in Fig. 2 shows a cyclic voltammogram of the platinum microdisc within the same solution. This exhibits a characteristic

---

[1] Defined as the upper frequency limit at which an AC signal is attenuated by 30%.

[2] Manufacturer quoted figure.

[3] The numerical solution of the RPNNP equation under similar conditions yields a maximum bubble radius of approximately 120 μm [5].
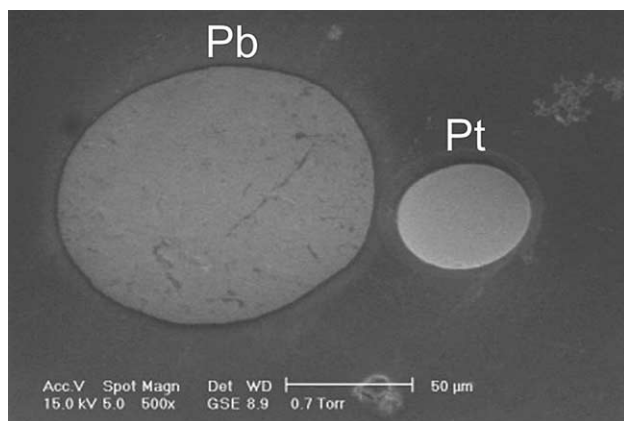
Fig. 1. SEM of the dual electrode. The lead microdisc (125 μm diameter) is on the left and the platinum microdisc (50 μm diameter) is on the right.
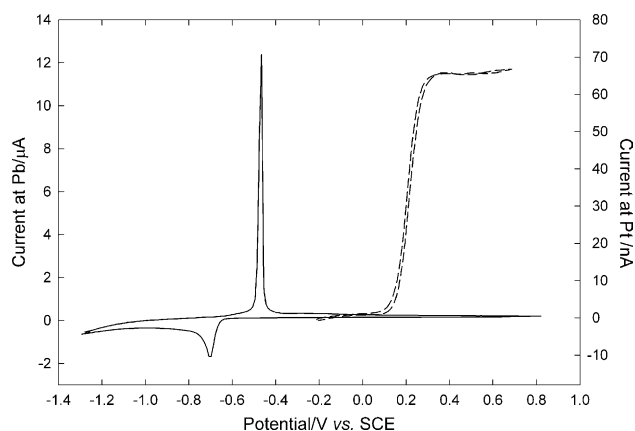


Fig. 2. Cyclic voltammogram of the 125 μm diameter lead disc (——) and 50 μm diameter platinum disc (– –) of the dual electrode in a solution containing 10 mM $K_4Fe(CN)_6$ and 0.75 M $Na_2SO_4$. For lead the sweep rate was 50 mV s$^{-1}$ and for platinum the sweep rate was 5 mV s$^{-1}$. Both experiments were performed under aerobic conditions at $25 \pm 1$ °C.
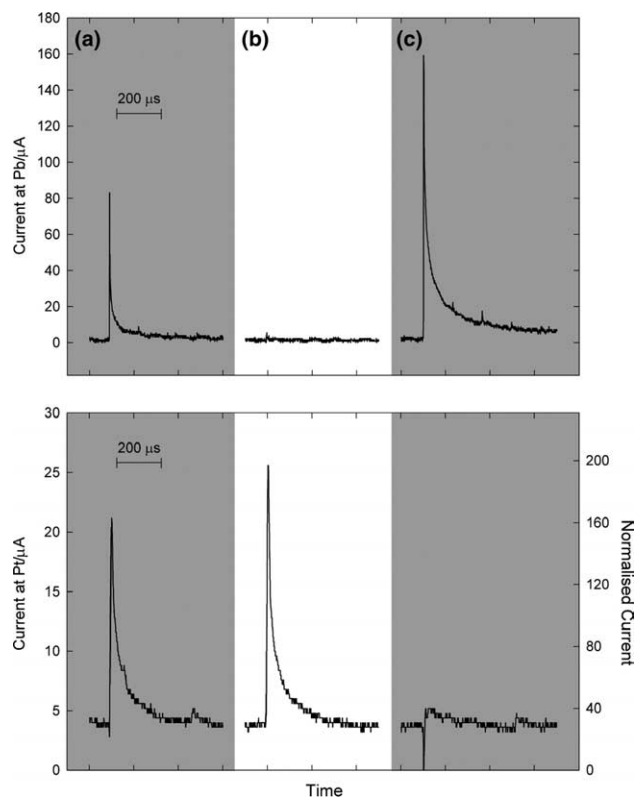


Fig. 3. Current traces from lead (125 μm diameter, upper plot) and platinum (50 μm diameter, lower plot) discs of the dual electrode under exposure to ultrasound. The electrode to horn separation was 1.4 mm. The solution contained 20 mmol dm$^{-3}$ $K_4Fe(CN)_6$ and 0.75 mol dm$^{-3}$ $Na_2SO_4$ and the experiment was performed under aerobic conditions at $25 \pm 1$ °C. Both electrodes were held at +0.8 V vs. Ag. The ultrasound frequency was 22.83 kHz and the power was $56 \pm 5$ W cm$^{-2}$. The mass transfer data has been normalised with respect to the steady-state current recorded under silent conditions (132 nA).

sigmoidal curve corresponding to the electro-oxidation of the $Fe(CN)_6^{4-}$ species on the platinum surface. A clear plateau (between +0.3 and +0.7 V vs. SCE) corresponds to the mass transfer limited oxidation of the $Fe(CN)_6^{4-}$ species.

For acoustoelectrochemical work the potential of both microdiscs was held at +0.8 V vs. Ag (a potential chosen to ensure mass transfer limitation on the platinum/$Fe(CN)_6^{4-}$ system and surface passivation on the lead system) and the electrode to horn separation was $1.40 \pm 0.02$ mm. Fig. 3 shows three different events recorded under the conditions stated above employing the dual microelectrode. The upper trace shows the current recorded at the passivated lead microelectrode ($i_{Pb/PbSO_4}$) and the lower trace is the current recorded at the platinum microelectrode for the oxidation of $Fe(CN)_6^{4-}$ ($i_{Pt/Fe(CN)_6^{4-}}$). In the case of the platinum microelectrode the current has also been normalised to

the silent steady state current of 132 nA (see right axis). In the section labelled (a), current transients are seen simultaneously on both traces. The magnitude and duration of the transients are in good agreement with previous work [2,6,8] and are indicative of an inertial bubble collapse, showing for the first time that both the mass transfer and erosion[4] effects of the same cavitation event can be recorded simultaneously. It is also

---

[4] It should be noted that enhanced dissolution of the $PbSO_4$ cannot account for the Pb transients observed. If one considers the solubility product of $PbSO_4$ ($1.82 \times 10^{-8}$) [14] then a surface concentration of $Pb^{2+}$ of $2.43 \times 10^{-11}$ mol cm$^{-3}$ can be calculated under the conditions stated. Considering that the rates of transient mass transfer can be assumed to be up to ~1 cm s$^{-1}$ this will approximate to a signal due to mass transfer enhanced dissolution of $5.8 \times 10^{-10}$ A. This is insignificant compared to the erosion transients observed (indeed five orders of magnitude smaller). In addition the erosion signal terminates at a defined distance between the source and the electrode whereas mass transfer effects vary over an extended distance. Hence, the transients observed for the Pb/$PbSO_4$ system are assumed (see later argument) to be attributable to inertial collapse and the associated erosion mechanisms. This is also supported by previous literature [8].

possible to detect cavitation events, which either produce mass transfer or erosion signals alone. Examples of these type of event are shown in Fig. 3(b) and (c), respectively. This clearly shows that the simultaneous current transients are genuine and not the result of coupling in the acquisition electronics. There is a minor transient, seen in the lower trace of part (c), which does not have the form of a mass transfer disturbance. However, coupling between the electrodes is insignificant on this scale and the overall current at the platinum electrode is dominated by genuine mass transfer events that occur. At times outside the occurrence of peaks there is a negligible current at the lead electrode, while at the platinum electrode there is a much increased current, up to ca. 30 times the silent steady-state current, due to deformation of the diffusion field by streaming processes. Assuming linear diffusion, analysis of this quasi-steady state current shows that the diffusion layer thickness under the sonication conditions used here is 0.7 μm.

Although the current time transients recorded simultaneously and shown in Fig. 3(a) are attributed to a single inertial cavitation event, they are probably the result of different effects associated with the collapse. Philipp and Lauterborn [15] showed that while microjets and associated shockwaves occur during the collapse of laser induced bubbles at a surface, the majority of the erosion observed is due to the generation of shockwaves. The resulting damage pattern is circular with a diameter of approximately 1.25 times the maximum bubble radius. It is assumed that these shockwaves cannot be detected in terms of increased mass transfer and the current spike at the platinum electrode must therefore be due to either an impinging microjet or the associated bubble motion and collapse that generated the erosive mechanism. There is no depletion in current prior to the mass transfer spikes shown in Fig. 3(a) and (b), suggesting that under these conditions the electrode is not blocked by the bubble prior to its collapse. The platinum electrode is effectively isolated from the lead owing to the small size of the diffusion layer and so it is clear that the effects of a collapse span a distance of at least 10 μm (see Fig. 1).

Mass transfer enhancement without associated erosion events (Fig. 3(b)) could be caused by non-inertial cavitation, which will occur in the region under investigation. However, mass transfer events of the magnitude and duration shown in the Fig. 3 ceased when the horn to electrode distance was increased to more than 1.5 mm. Non-inertial cavitation would still be expected at this distance; hence it is unlikely that the events shown in Fig. 3 are due to non-inertial bubble oscillation. At this time there is no obvious mechanism, which could explain an erosion event without mass transfer enhancement (Fig. 3(c)). There will certainly be a spatial effect whereby the response depends on the location of the bubble collapse. An inertial event at the extremity of the Pb/PbSO$_4$ electrode could be up to 160 μm from the centre of the Pt microdisc (see Fig. 1). At this distance the mass transfer signal associated with the inertial collapse is expected to be small compared to an event above the Pt microdisc centre. However, in addition shockwaves generated during cluster collapse should also be considered. This is discussed in depth elsewhere [16].

An SEM of the electrode following sonication is shown in Fig. 4, with the erosion of the lead clearly visible as a recessing of the surface (see Fig. 1). It is possible to calculate the area eroded in each event. The reader is directed to the details of the calculation which is reported elsewhere [8]. However, for the transients shown in Fig. 3(a) and (c) a pit radius of 8.6 or 16.8 μm, respectively, was obtained following the charge associated with the first 100 μs of the event. This is in close agreement with previous calculations [8].

The use of a lead/platinum dual electrode as described here has a number of advantages for the study of acoustoelectrochemistry. First, the microdiscs sample a relatively small volume of liquid and, as has been shown above, it is possible to detect the effects of a single bubble collapse. Second, the lead and platinum electrodes are sensitive to different physical processes associated with sonication. While the platinum microdisc can detect macroscopic fluid flow, bubble motions, inertial and non-inertial cavitation the passivated lead microdisc is only sensitive to high energy processes capable of surface erosion. Third, the use of sodium sulphate/potassium ferrocyanide electrolyte enables the microdiscs to be held at the same potential. This allows for far simpler acquisition electronics and minimises the effects of coupling between the two signals. Finally, the redox chemistry of the ferro/ferricyanide couple occurs in a potential range where the lead electrode is always passivated. This effectively allows the mass transfer response of the dual electrode to be 'turned on or off' by simply stepping the applied potential (between 0 and +0.8 V vs. Ag), without effecting the erosion detection. This
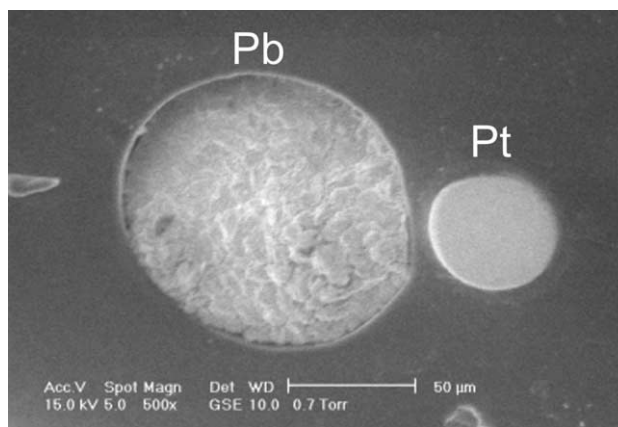


Fig. 4. SEM of the dual electrode following sonication for 500 s at a distance of 1.4 mm.

effect is illustrated clearly in Fig. 5, which shows current time traces recorded at much lower temporal resolution than those shown in Fig. 3. In the first 10 seconds the potential was held at +0.8 V vs. Ag and the ultrasound was off. As expected, no current was observed at the lead electrode, which is passivated and a steady-state anodic current was seen at the platinum electrode. The ultrasound was then switched on. At the lead electrode current transients due to repassivation were observed while an elevated quasi steady-state oxidation current was recorded at the platinum microdisc. When the potential was stepped to 0 V vs. Ag (20–30 s) the behaviour of the lead electrode was unaffected but the mass transfer current dropped to zero, as there is no redox chemistry occurring at the platinum electrode. On stepping the potential to −0.8 V vs. Ag (30–40 s) the erosion signal was lost due to the removal of the $PbSO_4$ layer. At the platinum electrode a large cathodic current was seen,

which is attributed to the reduction of hydrogen ions under enhanced mass transfer conditions. After the ultrasound was switched off (40–50 s) the current fell to a relatively small steady-state value.

It is important to note that the transients observed on the Pb electrodes are assumed to be caused by an erosion/corrosion mechanism and not by enhanced dissolution of the $PbSO_4$ layer as the result of bubble induced forced convection. This statement can be supported in a number of ways. First, the charge associated with the erosion events reported here is in the range 1.13–4.33 nC (measured over the first 100 μs Fig. 3(a) and (c)). This is large compared to what could be suggested for a dissolution based mechanism. Consider a scenario where mass transfer of fresh solution from the bulk effectively removed the local $Pb^{2+}$ concentration over an extended hemispherical distance of 250 μm in radius. The charge required to replace the $Pb^{2+}$ in this environment would be of the order of 0.15 nC. This is an order of magnitude less than the events recorded even excluding the unlikely nature of such a mechanism and ignoring the timescales of the processes involved. Second, such a dissolution mechanism relies on an extended dissolution volume. This assumption can be shown to be invalid by the construction and employment of a novel dual Pb/Pb electrode. In this case two 125 μm diameter Pb electrodes were sealed in epoxy and the erosion transients recorded simultaneously on exposure to cavitation. Fig. 6 shows the results of such an experiment. In most cases current–time transients are only observed on one of the two electrodes (see Fig. 6). Considering that the electrodes are only ∼20 μm apart (see insert SEM in Fig. 6), then an extended dissolution mechanism would sug-
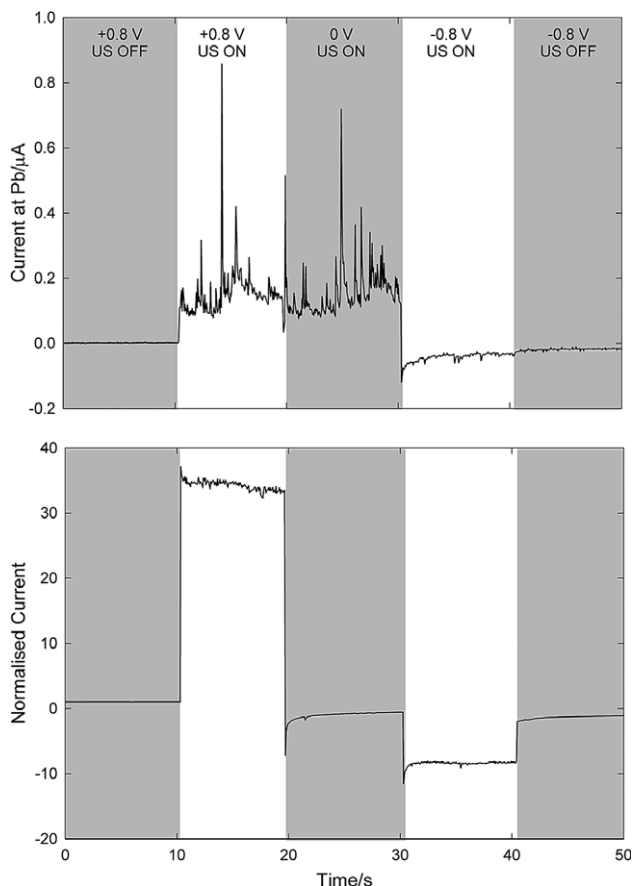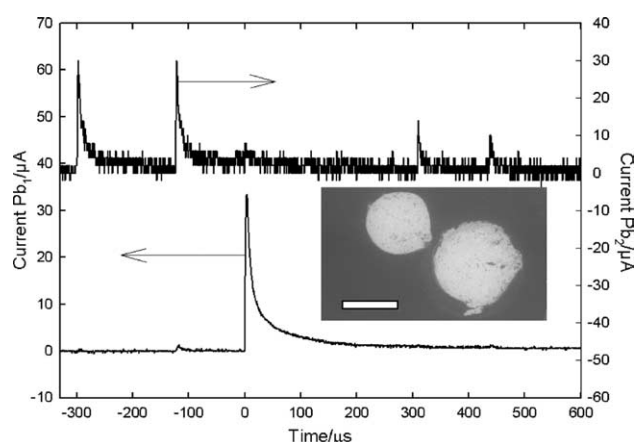


Fig. 5. Current–time traces from lead (125 μm diameter, upper plot) and platinum (50 μm diameter, lower plot) discs of the dual electrode under various experimental conditions recorded at low temporal resolution. The electrode to horn separation was 1.4 mm. The solution contained 20 mmol $dm^{-3}$ $K_4Fe(CN)_6$ and 0.75 mol $dm^{-3}$ $Na_2SO_4$ and the experiment was performed under aerobic conditions at 25 ± 1 °C. The ultrasound frequency was 22.83 kHz and the power was 56 ± 5 W $cm^{-2}$. The mass transfer data has been normalised with respect to the steady-state current recorded under silent conditions.



Fig. 6. Current–time traces recorded for a dual 125 μm Pb/Pb electrode exposed to cavitation. The solution contained 0.75 M $Na_2SO_4$. The potential was held at +0.8 V vs. Ag and the electrode to ultrasonic source distance was 1 mm. All other conditions as in Fig. 5. The insert shows an SEM of the dual electrode (scale bar = 100 μm). Note the noise associated with 'Current $Pb_2$' is caused by a low signal to noise for the fixed gain of the channel of the dual current follower employed.

gest that transients should be observed on both electrodes every time. This is clearly not the case suggesting that the mechanism producing the current–time transient is local and hence most probably originates in an erosive event. Third, for a dissolution mechanism to be responsible for current–time transients it is necessary to have a concentration gradient of $Pb^{2+}$ from the electrode to the solution. However, when experiments were performed with a $Pb^{2+}$ saturated solution current–time transients of the form shown in Fig. 3 (and in agreement with previous literature [8]) were observed. This last set of experiments, the set of calculations reported here and elsewhere proves that the current–time transients observed for the Pb system are most likely associated with an erosion based mechanism but cannot be associated with dissolution of the $PbSO_4$ layer.

## 4. Conclusions

It has been shown that the simultaneous recording of the erosion and mass transfer effects associated with an inertial cavitation event can be achieved using this dual microelectrode system. Further work aims to broaden the region under investigation to include areas further from the ultrasonic horn where periodic mass transfer enhancement due to non-inertial cavitation has been reported [11,12]. These electrochemical results will be used in conjunction with sonoluminescent and sonochemiluminescent imaging, high-speed photography, and acoustic measurements to build a complete picture of the environment in the vicinity of an operating ultrasonic horn.

## References

[1] J. Klima, C. Bernard, C. Degrand, J. Electroanal. Chem. 399 (1995) 147.
[2] F.J. Del Campo, J. Melville, J.L. Hardcastle, R.G. Compton, J. Phys. Chem. A 105 (2001) 666.
[3] J.P. Lorimer, B. Pollet, S.S. Phull, T.J. Mason, D.J. Walton, U. Geissler, Electrochim. Acta 41 (1996) 2737.
[4] C.R.S. Hagan, L.A. Coury, Anal. Chem. 66 (1994) 399.
[5] P.R. Birkin, S. Silva-Martinez, J. Electroanal. Chem. 416 (1996) 127.
[6] P.R. Birkin, S. Silva-Martinez, J. Chem. Soc., Chem. Commun. (1995) 1807.
[7] S.A. Perusich, R.C. Alkire, J. Electrochem. Soc. 138 (1991) 708.
[8] P.R. Birkin, R. O'Conner, C. Rapple, S. Silva-Martinez, J. Chem. Soc., Faraday Trans. 94 (1998) 3365.
[9] G.O.H. Whillock, B.F. Harvey, Ultrasonics Sonochemistry 4 (1997) 33.
[10] P.R. Birkin, T.G. Leighton, Y.E. Watson, J.F. Power, Acoust. Bull. 26 (2001) 24.
[11] E. Maisonhaute, B.A. Brooks, R.G. Compton, J. Phys. Chem. B 106 (2002) 3166.
[12] E. Maisonhaute, P.C. White, R.G. Compton, J. Phys. Chem. B 105 (2001) 12087.
[13] T.G. Leighton, The Acoustic Bubble, Academic Press, London, 1994.
[14] D.R. Lide (Ed.), Handbook of Chemistry and Physics 1913–1995, CRC Press, Boca Raton, FL, 1995.
[15] A. Philipp, W. Lauterborn, J. Fluid Mech. 361 (1998) 75.
[16] P.R. Birkin, D.G. Offin, T.G. Leighton, in preparation.